Journal of Research and Applications in Mechanical Engineering
ISSN: 2229-2152 (Print); 2697-424x (Online)
(2023) Vol. 11, No. 2, Paper No. JRAME-23-11-008
[DOI: 10.14456/jrame.2023.8]

Research Article

Flow-Direction Control of Primary Jets Near a Wall Boundary Using Secondary Flow with a Coanda Surface

H. Tezuka[1,*]
Q. Zhang[1]
K. Nishibe[2]
K. Sato[3]
[1]*Mechanical Engineering Program in the Graduate School of Engineering, Kogakuin University, Tokyo 192-0046, Japan*
[2]*Department of Mechanical Engineering, Tokyo City University, Tokyo 158-8557, Japan*
[3]*Department of Mechanical System Engineering, Kogakuin University, Tokyo 192-0046, Japan*

Received 20 January 2023
Revised 20 April 2023
Accepted 2 May 2023

Abstract:
Fluidic thrust vectoring, a method for controlling jet direction with no moving parts, has attracted attention as it does not require changing the geometry of the device, thus reducing the number of parts in the device. The application of synthetic jets as secondary flows has recently been proposed to adjust the deflection angle arbitrarily. However, studies regarding the relationship between the plane wall boundary and the flow characteristics of jets while applying fluidic thrust vectoring are scarce. In this study, we applied synthetic jets generated by a speaker to a secondary flow with a Coanda surface. We elucidated the influence of the oscillation characteristics of the secondary flow on the deflection angle of the primary jets near a plane wall. By adjusting the dimensionless frequency, the jet deflects toward the opposite side of the plane wall surface, even for the jet near the plane wall surface. In this condition range, we can set the maximum jet deflection angle to approximately 20 deg when the momentum ratio between the primary and secondary flow at slot is 0.08 and dimensionless frequency 0.11.

Keywords: *Jet vectoring, Coanda effect, Secondary flow, Synthetic jets, Frequency*

1. Introduction

The method of controlling the direction of a primary jet by a secondary flow is called fluidic thrust vectoring and has been investigated extensively. In general, fluidic thrust vectoring is implemented by adjusting the secondary flow momentum generated near the cylinder surface [1-12]; a large deflection angle can be achieved. This method was originally proposed in the field of aeronautics [1-5] and is expected to save energy and improve the performance of next-generation aircraft in the development of tail wings. Mason and Closer [1] used an injection jet as a secondary jet to study the effect of the momentum ratio between the primary jet and secondary flow on the jet deflection characteristics by conducting experiments and CFD analysis. The results show that using the injection flow as a secondary flow can provide a good deflection ability. The "dead zone" region can be narrowed at certain shape parameters. Kobayashi et al. [3] proposed a method using a synthetic jet as the secondary flow. They reported that the deflection angle of the jets depended on the momentum ratio between the primary and secondary jets and the dimensionless frequency of the synthetic jets. Recently, Tamanoi et al. [8, 9] discussed the effect of jet width on jet deflection characteristics as a fundamental study of fluidic thrust vectoring. The effects of the co-flow and counterflow near the Coanda surface on the deflection characteristics of the primary jet using different momentum

* Corresponding author: H. Tezuka
E-mail address: am22042@ns.kogakuin.ac.jp

ratio, jet widths, etc., were parametrically investigated. The results showed that the degree of jet deflection depended on the jet width when the secondary flow was a counterflow. However, the jet width did not affect the deflection angle when the secondary flow was a co-flow.

Despite the aforementioned research, few studies have investigated the effects of wall surfaces on the flow characteristics of jets when synthetic jets are used as secondary flows. The phenomenon of jets near a wall being attracted to a wall surface [13, 14] is a basic jet flow characteristic widely known as the Coanda effect. In actual situations, boundaries are ubiquitous; often, boundaries exist in the vicinity of the jets. For example, there are ceilings and sidewalls near air conditioner vents in a room and blades and shrouds near the slots for jets when casing treatments are performed in fluid machinery. In such cases, interference between jets and wall boundaries is a significant issue that must be resolved when attempting to control the direction of jets. A significant problem must be solved: the interference between the jets and wall boundaries for the jet deflection control.

As the first step to solve the aforementioned problem, this study attempts to control the flow characteristics of the reattached flow to the plane wall due to the Coanda effect by the secondary synthetic jet in addition to steady injection and suction flow with a cylindrical Coanda surface in the case of a certain geometry (offset ratio and plane wall length) conditions. Applying a secondary flow showed that the jet attracted to the plane wall can be deflected to the opposite side of the plane wall. We also discuss the influence of the dimensionless frequency on the jet deflection characteristics under the condition of a certain momentum ratio.

2. Experimental Methods

Figure 1 shows the schematic of the experimental apparatus. The working fluid in this experiment was air, and we applied a continuous jet as the primary flow. Figures 1(a) and 1(b) show the apparatus configuration when the secondary flow was steady (continuous jet or continuous suction) and a synthetic jet, respectively. We generated the primary jet and steady secondary flow using blowers (U75-2-R313 and U2V-70S, Showa Electric Co.). A steady secondary flow was generated on the opposite plane wall side with injection and suction using a vortex-type blower (U2V-70S, manufactured by Showa Electric Co.). We switched the injection and suction modes of the secondary flow by exchanging the discharge and suction ports of the blower. We then generated the secondary synthetic jet using a signal generator, amplifier (Classic Pro V3000), and speaker (DIECOOK DD-15L). We supplied a secondary flow after injecting the primary jet and developing the flow field sufficiently. The flow field in the test section was sandwiched between two acrylic plates with dimensions of 1.0 m × 1.0 m in the x-y plane and 7.0×10^{-2} m along the z-axis. The length of the wall surface and the distance from the centerline of the slot to the wall surface were set to 2.5×10^{-1} m and 5.0×10^{-2} m, respectively, referring to the analysis results by Borque and Newman [13].

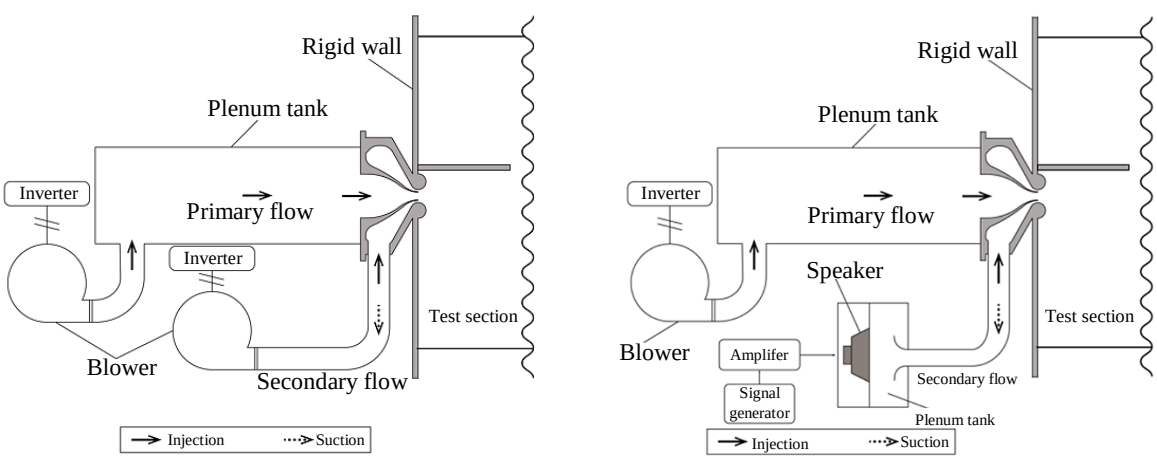

(a) Schematic of the experimental apparatus for continuous secondary flow

(b) Schematic of the experimental apparatus for secondary synthetic jet

Fig. 1. Schematic of experimental apparatus

Figure 2 shows a magnified view of the slot geometry. The slot widths h_1 and h_2 of the primary and secondary jets are 1.0×10^{-2} m and 2.0×10^{-3} m, respectively, and the slot width ratio is constant at $h_2 / h_1 = 0.2$. The direction of the jet flow was controlled by interfering with the primary jet and secondary flow and installing a cylindrical Coanda surface with a radius $R = 1.5 \times 10^{-2}$ m and a flat plate wall of 2.5×10^{-1} m length in the vicinity of the jet. In this study, we measured the representative velocities of the primary and secondary flows U_1 and U_2 at the slot center of its width and span. U_1 at 8 m/s. To obtain values of M_2 / M_1 of 0.08, U_2 was tested at 5.06 m/s. The dimensionless frequencies, f^*, are 1.3×10^{-2}, 3.8×10^{-2}, 6.3×10^{-2}, 8.9×10^{-2}, and 1.1×10^{-1}. This experiment was conducted under fixed geometric conditions. The Reynolds number, *Re*, based on the primary jet velocity U_1 and slot width h_1 is considered $Re = 5.3 \times 10^3$. The velocity of the secondary synthetic jet is expressed as Equation (1) [3]:

$$U_2 = \sqrt{\frac{1}{T}\int_0^T U_A^2 \sin^2 \frac{2\pi}{T} t dt} \tag{1}$$

Velocity measurements were performed at the center of the slot outlet using an I-type probe (Kanomax 0251R-T5) on a hot-wire anemometer (Kanomax Smart-CTA 7250). The probe was placed parallel to the z-axis. For the velocity measurement, we confirmed that the deviation from the calibration curve was within 1.6%, with a velocity range of 2.9–15 m/s.

In addition, the maximum time resolution of the hot-wire anemometer was 20 kHz, and we measured it at 10 kHz. Therefore, the time resolution was sufficient compared with the time characteristics of the flow fluctuation. In the visualization experiment, the smoke generated by a smoke generator was introduced through the blower inlet of the primary flow. A halogen light was used as the light source downstream from the jets and captured these phenomena using a digital camera (SONY VLOGCAM ZV-1) operating at 480 fps. In the velocity distribution measurement experiment, the velocity distribution $|\boldsymbol{v}| = \sqrt{u^2 + v^2}$ on a circular arc of radius $r_m = 1.5 \times 10^{-1}$ from the slot center (origin) was measured at 2° intervals in the range $-18° \leq \theta \leq 90°$. For the deflection angle calculation method, assuming that $|v| > 0.3\,|U_{max}|$ is a distinct jet structure, the flow center is calculated as an integral over the range from θ_a to θ_b, and the angle corresponding to the flow center is defined as the jet deflection angle θ_C, as in Equation (2) [15].

$$\theta_C = \frac{1}{\int_{\theta_a}^{\theta_b} |v| d\theta} \int_{\theta_a}^{\theta_b} |v| \theta \, d\theta \tag{2}$$

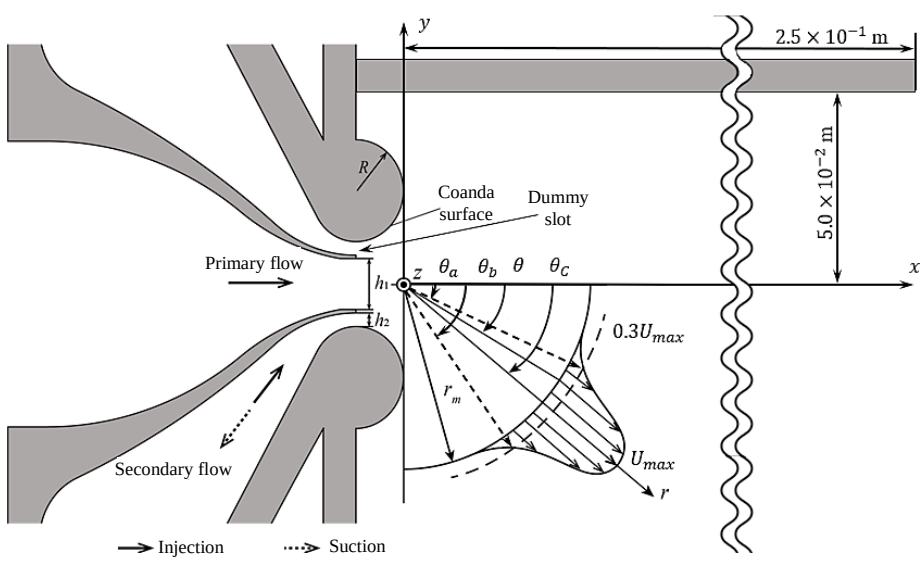

Fig. 2. Geometric shape of slot

3. Results and Discussion

Figures 3-5 show examples of the visualized jet behavior near a wall surface with an offset ratio of 5.0. Figure 3 shows only the primary jet (no secondary jet). Under these conditions, the jets are attracted to the wall surface owing to the Coanda effect caused by the flat wall surface, indicating that the jet was attached to the wall near $x / h_1 = 25$. This result is in close agreement with the experimental results obtained in previous studies [13, 14].

Figures 4 and 5 show examples of the observed behavior when the secondary flow is activated with a momentum ratio of $M_2 / M_1 = 0.08$. Figure 4 shows the case of steady secondary flow under the (a) injection and (b) suction conditions. Figure 5 shows the behavior when the secondary flow is a synthetic jet: (a) for $f^* = 1.3 \times 10^{-2}$ and (b) for $f^* = 1.1 \times 10^{-1}$.

In Figure 4 (a), in the jets are attracted toward the wall under the secondary flow jet condition, and the reattachment point distances were approximately the same as those in Fig. 3. This result corresponds to the fact that this condition was located within the dead zone in a previous study. However, under condition (b), where the secondary flow is a suction flow, the jet is deflected toward the antiplate wall. Under these conditions, the suction caused a pressure drop near the cylinder, suggesting that the Coanda effect is due to the cylinder being larger than that due to the flat plate wall.

Figure 5 shows a typical flow pattern when the secondary flow is a synthetic jet. Figures 5(a) and 5(b) were captured under the typical low-frequency condition $f^* = 1.3 \times 10^{-2}$ and typical high-frequency condition $f^* = 1.1 \times 10^{-1}$, respectively. In the low-frequency condition (a), the jet is slightly deflected toward the antiplate side but generally flows parallel to the x-axis. In contrast, in the high-frequency condition (b), the jet is significantly deflected toward the antiplate side, indicating that the direction of the jet can be controlled by the cylindrical Coanda surface and secondary flow even when the plate wall exists near the slot and that the degree of deflection can be adjusted by the dimensionless frequency when the secondary flow is a synthetic jet.

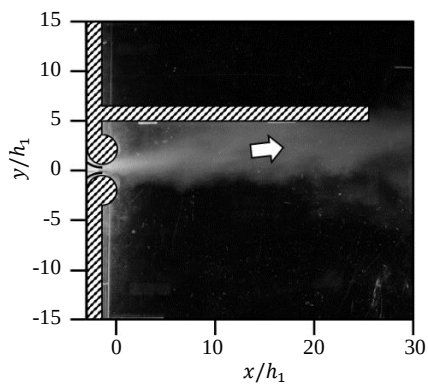

Fig. 3. Visualization of flow patterns using only primary jet
($h_1 = 1.0 \times 10^{-2}$ m, $U_1 = 8$ m/s)

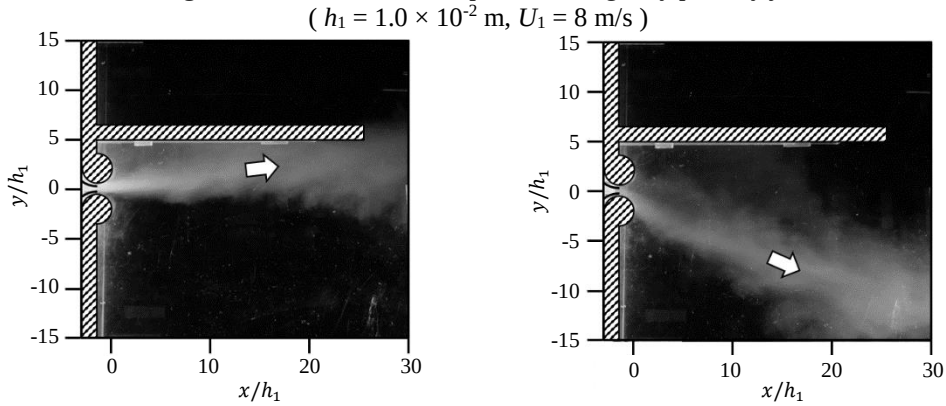

(a) Injection (b) Suction

Fig. 4. Visualization of flow patterns for continuous flow as the secondary flow under the condition of $M_2 / M_1 = 0.08$ ($h_1 = 1.0 \times 10^{-2}$ m, $h_2 = 2.0 \times 10^{-3}$ m, $U_1 = 8$ m/s, $U_2 = 5.06$ m/s, $Re = 5.3 \times 10^3$)

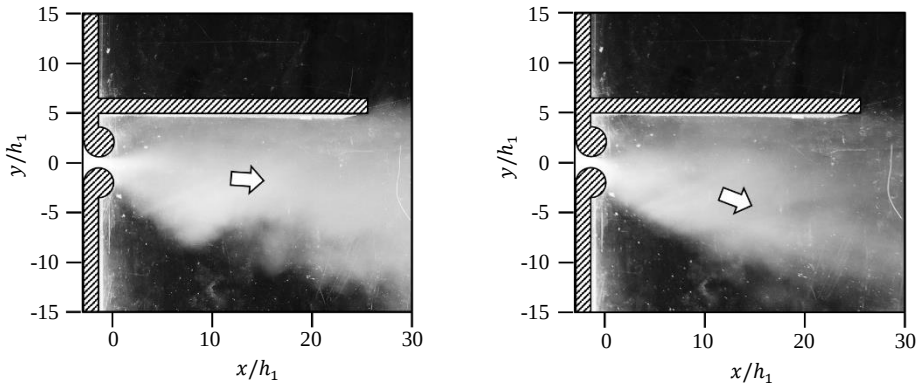

(a) $f^* = 1.3 \times 10^{-2}$ ($f = 10$ Hz) (b) $f^* = 1.1 \times 10^{-1}$ ($f = 90$ Hz)

Fig. 5. Visualization of flow patterns for synthetic jet as the secondary flow under the condition of $M_2 / M_1 = 0.08$ ($h_1 = 1.0 \times 10^{-2}$ m, $h_2 = 2.0 \times 10^{-3}$ m, $U_1 = 8$ m/s, $U_2 = 5.06$ m/s, $Re = 5.3 \times 10^3$)

Figure 6(a) shows the time-averaged velocity distribution measured on the arc for the momentum ratio $M_2 / M_1 = 0.08$ under the same geometric conditions as those shown in Figs. 3-5. The conditions of the primary flow alone and the injection jet as the secondary flow showed similar velocity profiles. The jet deflection is greatest when the secondary flow is under steady suction. The results also show that the angle θ of the jet center position (the angle of maximum velocity) increases with increasing dimensionless frequency f^* when a synthetic jet is used for the secondary flow.

Figure 6(b) shows the relationship between the deflection angle θ_C and the dimensionless frequency f^*. The secondary suction flow exhibited the best deflection ability. Moreover, the deflection angle θ_C increases as the dimensionless frequency of secondary synthetic jets f^* increases, confirming that the deflection angle θ_C depends on the dimensionless frequency f^*.

Jets near the plane wall are generally attracted to the plane wall side because of the Coanda effect. However, the above results indicate that the direction of the jet near the plane wall can be controlled on the opposite side of the plane wall by applying steady suction or a synthetic jet to the secondary flow. In particular, the deflection angle can be adjusted using the dimensionless frequency when the secondary flow is the synthetic jet.

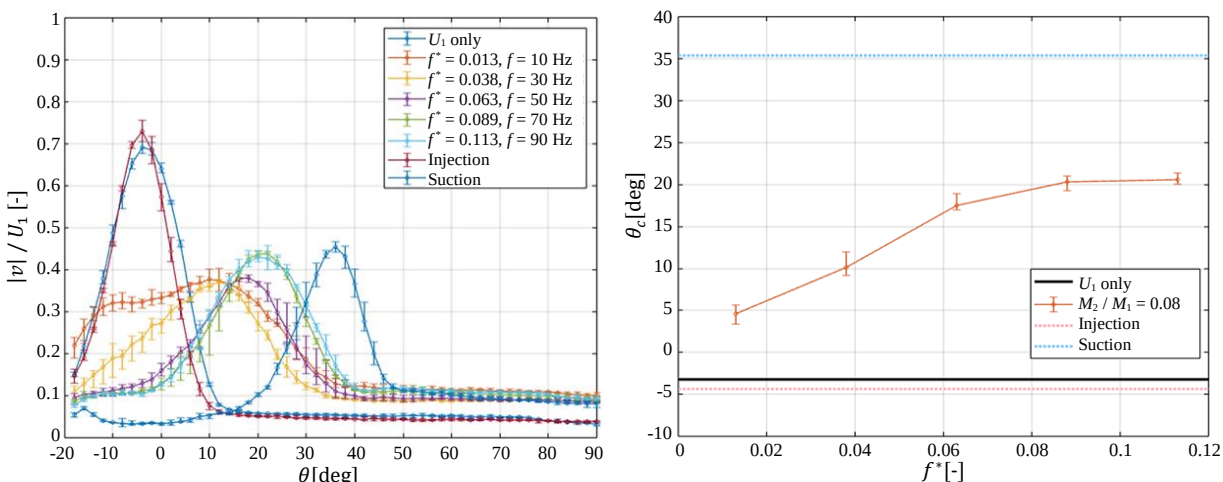

(a) Dimensionless time-averaged velocity distributions (b) Relationship between dimensionless frequency and deflection angle

Fig. 6. Velocity distribution and deflection angle for various dimensionless frequency f^* under the condition of $M_2 / M_1 = 0.08$

4. Conclusion

In this study, steady injection, steady suction, and synthetic jets were applied to the secondary flow with a cylindrical Coanda surface to elucidate the flow characteristics of jets near a plane wall.

1. The deflection angle of the jet near the plane wall can be controlled by a steady secondary flow of the suction and secondary synthetic jets, which can deflect the jet toward the opposite side of the plane wall under certain conditions.
2. The jet deflection characteristics depend on the dimensionless frequency f^* of the synthetic jet under the shape parameters used in this study.
3. The jet-deflection characteristics depend on the dimensionless frequency f^*. Under the present geometric condition, the direction of the jet can be controlled up to approximately 20 ° when the synthetic jet is set in the secondary flow with a momentum ratio $M_2/M_1 = 0.08$.

Nomenclature

f	:	Frequency [Hz]
f^*	:	Dimensionless frequency (= fh_1/U_1) [-]
h_1	:	Primary slot width (= 1.0×10^{-2}) [m]
h_2	:	Secondary slot width (= 2.0×10^{-3}) [m]
M	:	Momentum of primary or secondary flow at slot exit (= $\rho U^2 h$) [N]
R	:	Radius of Coanda surface (= 1.5×10^{-2}) [m]
Re	:	Reynolds number (= $U_1h_1/\nu = 5.3\times10^3$) [-]
r_m	:	Radius of velocity measurement arc (= 1.5×10^{-1}) [m]
t	:	Time [s]
T	:	Period of velocity oscillation (= $1/f$) [s]
u	:	Velocity in the x-direction [m/s]
U	:	Velocity of primary or secondary flow at slot exit [m/s]
U_A	:	Amplitude of velocity oscillation for secondary synthetic jet [m/s]
U_{max}	:	Maximum velocity of velocity distribution[m/s]
v	:	Velocity in the y-direction [m/s]
$\|\boldsymbol{v}\|$	:	Absolute value of the velocity at an arbitrary point [m/s]
x, y, z	:	Coordinate axes
z_h	:	Height of test section (=7.0×10^{-2}) [m]
θ	:	Clockwise angle from x-axis [deg]
θ_a	:	Angle of the first point of intersection between $0.3U_{max}$ and velocity distribution [deg]
θ_b	:	Angle of the second point of intersection between $0.3U_{max}$ and velocity distribution [deg]
θ_C	:	Jet deflection angle [deg]
ν	:	Kinematic viscosity (=1.5×10^{-5}) [m^2/s]
ρ	:	Fluid density [kg/m^3]

Subscripts

1	:	Primary jet
2	:	Secondary jet

Acknowledgments

We thank Mr. Minoru Nakagawa (Kogakuin University) for his assistance in conducting this study, Mr. Yuki Watanabe, and Mr. Yu Tamanoi (Kogakuin University graduate students) for their assistance in fabricating the experimental apparatus. We would like to thank Editage (www.editage.com) for English language editing. We express our gratitude to them.

References

[1] Mason MS, Crowther WJ. Fluidic thrust vectoring of low observable aircraft. CEAS Aerospace Aerodynamic Research Conference; 2022 Jun 10-12; Cambridge, UK. p. 1-17.

[2] Trancossi M, Stewart J, Subhash M, Angeli D. Mathematical model of a constructal Coanda effect nozzle. J Appl Fluid Mech. 2016;9(6):2813-2822.

[3] Kobayashi R, Watanabe Y, Tamanoi Y, Nishibe K, Kang D, Sato K. Jet vectoring using secondary Coanda synthetic jets. Mech Eng J. 2020;7(5):1-17.

[4] Hunter CA, Deere KA. Computational investigation of fluidic counterflow thrust vectoring. 35th AIAA/ASME/SAE/ASEE Joint Propulsion Conference & Exhibit; 1999 Jun 20-23; Los Angeles, United State. p. 1-14.

[5] Al-Asady A, Abdullah AM. Fluidics thrust vectoring using co-flow method. Al-Nahrain J Eng Sci. 2017;20(1):5-18.

[6] Watanabe Y, Sato K, Sato M, Nishibe K, Kang D, Yokota K. Vector control of jet flow using secondary excited jets. The 29th International Symposium on Transport Phenomena; 2018 Oct 30 - Nov 2; Honolulu, United States.

[7] Tamanoi Y, Watanabe Y, Kobayashi R, Sato K. Control of jet flow direction. Proceedings of the 57th Annual Meeting of the Hokkaido Branch; 2020 Mar 7; Hokkaido, Japan. Japan: Japan Society of Mechanical Engineers; 2020. p. 29-30. (In Japanese)

[8] Tamanoi Y, Watanabe Y, Kobayashi R, Sato K. Jet direction control using secondary flows. J Phys: Conf Ser. 2021;1909:012040.

[9] Tamanoi Y, Sato K. Structure of jet deflected by secondary flow. International Symposium on Advanced Technology; 2021 Jan 14; Los Baños, Philippines.

[10] Tamanoi Y, Kobayashi R, Sato K, Nishibe K, Kang D. Flow control using excited jets with Coanda surfaces. The 31st International Symposium on Transport Phenomena; 2020 Oct 13-16; Honolulu, United States.

[11] Tezuka H, Nakagawa M, Tamanoi Y, Sato K. Direction control of primary jets using secondary flow near boundaries. Proceedings of the 28th Annual Meeting of the Kanto Branch of the Japan Society of Mechanical Engineers; 2022 Aug 7; Kanto, Japan. (In Japanese)

[12] Zhang Q, Tamanoi Y, Kang D, Nishibe K, Yokota K, Sato,K. Influence of amplitude of excited secondary flow on the direction of jets. Trans Japan Soc Aero Space Sci. 2023;66(2):37-45.

[13] Borque C, Newman BG. Reattachment of a two-dimensional, incompressible jet to an adjacent flat plane. Aeronaut Quart. 1960;11(3):201-232.

[14] Shakouchi T. Jet flow engineering fundamentals and applications. Tokyo: Morikita Publishing; 2009. (In Japanese)

[15] Zhang Q, Takahashi F, Sato K, Tsuru W, Yokota K. Jet direction control using circular cylinder with tangential blowing. Trans Japan Soc Aero Space Sci. 2021;64(3):181-188.